

Thickness determination of MoS₂, MoSe₂, WS₂ and WSe₂ on transparent stamps used for deterministic transfer of 2D materials

Najme S. Taghavi^{1,2}, Patricia Gant¹(✉), Peng Huang^{1,3}, Iris Niehues⁴, Robert Schmidt⁴, Steffen Michaelis de Vasconcellos⁴, Rudolf Bratschitsch⁴, Mar García-Hernández¹, Riccardo Frisenda¹(✉), Andres Castellanos-Gomez¹(✉)

¹ Materials Science Factory, Instituto de Ciencia de Materiales de Madrid (ICMM), Consejo Superior de Investigaciones Científicas (CSIC), Sor Juana Inés de la Cruz 3, 28049 Madrid, Spain.

² Faculty of Physics, Khaje Nasir Toosi University of Technology (KNTU), Tehrān 19697 64499, Iran.

³ State Key Laboratory of Tribology, Tsinghua University, Beijing 100084, China.

⁴ Institute of Physics and Center for Nanotechnology, University of Münster, 48149 Münster, Germany.

Address correspondence to Patricia Gant (patricia.gant@csic.es), Riccardo Frisenda (riccardo.frisenda@csic.es) and Andres Castellanos-Gomez (andres.castellanos@csic.es)

ABSTRACT

Here, we propose a method to determine the thickness of the most common transition metal dichalcogenides (TMDCs) placed on the surface of transparent stamps, used for the deterministic placement of two-dimensional materials, by analyzing the red, green and blue channels of transmission-mode optical microscopy images of the samples. In particular, the blue channel transmittance shows a large and monotonic thickness dependence, making it a very convenient probe of the flake thickness. The method proved to be robust given the small flake-to-flake variation and the insensitivity to doping changes of MoS₂. We also tested the method for MoSe₂, WS₂ and WSe₂. These results provide a reference guide to identify the number of layers of this family of materials on transparent substrates only using optical microscopy.

MANUSCRIPT TEXT.

Since the isolation of graphene in 2004[1], the mechanical exfoliation method (also called Scotch tape method) has established itself as one of the most used techniques to produce 2D materials [2–5]. Its facile implementation combined with the high quality of the produced samples are most likely the reasons behind the success of this technique. Mechanical exfoliation, nonetheless, yields randomly distributed flakes of various thicknesses and sizes on the surface of the substrate. This limitation has been overcome to a great extent through the development of rapid methods to find and identify thin flakes based on the observation of the apparent color when they are transferred onto a SiO₂/Si surface [6–12]. On this substrate, there is a dependency of the apparent color of the flake with its thickness due to thin-film interference effects and many

epi-illumination (reflection mode) microscopy-based methods have been developed to identify 2D materials and to determine their number of layers [6–12]. An alternative way to overcome the limitations of mechanical exfoliation relies on the use of experimental tools that allow for the deterministic placement of flakes onto any desired sample position with micrometer accuracy [13–19]. These transfer techniques opened the field of van der Waals heterostructures [18,20–23]. To carry out the deterministic placement, the isolated flakes have to be deposited onto the surface of a polymer-based stamp that is used as a release layer or sacrificial carrier substrate. These stamps are made of transparent material to allow for the accurate alignment of the flake to be transferred with the acceptor surface by inspection with an optical microscope. Unfortunately, on the surface of the transparent stamps most of the previously developed optical identification methods, based on the apparent colors, are less straightforward to implement and less effective and other complementary techniques such as Raman or photoluminescence (which are slower and more complex than simple optical microscopy) are typically used to determine the number of layers of the flakes deposited on the polymeric stamps [24–27]. Due to the increasing interest on the use of deterministic placement methods to assemble nanodevices and van der Waals heterostructures, the development of alternative methods to determine the thickness of 2D materials on the surface of the transparent polymeric stamps is extremely relevant for the 2D community. That is exactly the goal of this work, to provide a fast and reliable method to identify TMDC flakes on transparent polymeric stamps and to determine their number of layers.

Here, we demonstrate that the quantitative analysis of transmission optical mode images of TMDC flakes on the surface of transparent polydimethylsiloxane (PDMS) stamps is a reliable method to accurately determine their thickness. We compare the results of the quantitative analysis of the transmission mode optical images with results obtained via micro-reflectance spectroscopy [28], photoluminescence and Raman spectroscopy to verify its reliability. In order to test the limitations of this method, we probe its sensitivity concerning the doping level of the sample by measuring MoS₂ samples with different intentional doping. We found that the determination of the thickness with the analysis of transmission mode images is rather independent on the doping level, giving similar results for all the studied samples. Finally, we extended the study to other TMDCs to provide a reference guide to identify the number of layers of this family of materials. As the measurement of the transmittance is a differential measurement, the effect of the substrate is accounted for and thus these results could be extrapolated to other transparent stamp surfaces like poly(methyl methacrylate) (PMMA) or polycarbonate/hexagonal boron-nitride (PC/hBN).

Figure 1a shows a transmission mode optical microscopy image of a MoS₂ flake transferred onto a Gel-Film substrate (a commercially available polydimethylsiloxane film, by Gel-Pak) which is typically used as a stamp for deterministic dry transfer of 2D materials [16,29]. Figure 1b displays line profiles of the intensity of the red, green and blue channels extracted from the image in Figure 1a. The transmittance of the different channels is calculated by normalizing the red, green and blue (RGB) channel images to the intensity of these channels measured on the bare substrate. From the line profiles, one can see that the transmittance of each channel changes stepwise with the number of layers. To determine the feasibility of using the transmittance to determine the number of layers one needs to characterize the statistical variations of the transmittance in different MoS₂ flakes and the uncertainty associated to these measurements. Therefore, we acquired transmission mode optical microscopy images of 202 MoS₂ flakes and we compiled three histograms by binning the measured transmittance of the flakes for each color channel. Figure 1c shows the histograms of the red, green and blue channels plotted versus 1-transmittance. Although all the histograms display prominent

peaks that correspond to different number of layers, the histogram of the blue channel shows a larger separation between the peaks (while maintaining a similar peak width) making it easier to distinguish between 1, 2, 3 or 4 layers of MoS₂. The higher contrast of the blue channel is expected as MoS₂ (and MoSe₂, WS₂ and WSe₂ as well) present a strong excitonic feature (sometimes referred to as C exciton in the literature) in the blue part of the spectrum that yields a strong optical absorption in that wavelength range.[30,31]

In order to verify the reliability of this method to determine the number of layers we benchmarked it with other commonly used spectroscopic techniques. In Figure 2a the experimental data employed to build up the histogram in Figure 1c is displayed in a scatter plot. We have selected 4 flakes with different thickness in the range between 1 layer and 4 layers, respectively labeled as 1L, 2L, 3L and 4L accordingly to their blue channel transmission, and we have carried out micro-reflection, Raman and photoluminescence measurements to have three independent methods to determine the thickness. Figure 2b shows the differential reflectance spectra acquired on these flakes where the intensity and the energy of the A exciton monotonically changes from 1L to 4L. The intensities and exciton positions obtained in the spectra agree with the values expected for 1L to 4L,[31] which means a correct assignment of the thickness estimated by the blue channel values [32]. Figure 2c compares the Raman spectra measured on the same flakes (vertically displaced by 0.1 for clarity) with a 532 nm excitation laser. We verify the number of layers of the samples from the difference between the A_{1g} and E¹_{2g} phonon [33,34] energies in Raman and check again the accuracy in the determination of the number of layers using the blue channel transmittance. Figure 2d shows photoluminescence measurements for 1L, 2L, 3L and 4L flakes, also measured with a 532 nm excitation laser. The intensity and the position of the A exciton dramatically depends on the number of layers and it confirms that the assignment of number of layers determined by the blue channel transmission is reliable.[35,36]

We further test the analysis of the blue channel transmission images by studying MoS₂ samples synthesized with intentional substitutional metal atoms at the Mo sites to enquiry about the robustness of this technique against a moderate variation of the chemical composition that lead to a big change in the electronic properties.[37,38] We follow the synthesis method described in references [37–40] for the growth of Fe-doped, Ni-doped, Nb-doped and Co-doped MoS₂ crystals. In all cases a 0.5% of dopant material has been added in the ampoule for the synthesis of these doped MoS₂ samples which lead to a final doping level in the 0.3-0.4% range. Figure 3 compares the histograms of the blue channel transmittance constructed by analyzing 50 flakes of each doped MoS₂ material. This comparison clearly illustrates how our method is rather insensitive to variations of the chemical composition (that induces strong changes in the doping level of the material). We note that other optical spectroscopic methods to determine the thickness of transition metal dichalcogenides such as Raman and photoluminescence spectroscopy are strongly dependent on the doping level of the samples and on slight variations of the chemical composition.[41–45]

We extended this method to other 2D materials of the TMDCs family to provide a general guide to identify these materials through the analysis of the blue channel of transmission images. Figure 4 compares the blue channel transmission histograms built up after analyzing 202 MoS₂ flakes, 200 MoSe₂ flakes, 200 WS₂ flakes and 200 WSe₂ flakes. In all the cases the histograms show well-resolved peaks indicating that one can unambiguously determine the number of layers through the quantitative analysis of the blue channel of the transmission mode optical images.

In summary, we have introduced a very simple and fast yet reliable method to determine the number of layers of MoS₂, MoSe₂, WS₂ and WSe₂ deposited on a PDMS stamp, used for deterministic placement of 2D materials. Moreover, being a differential measurement, the effect of the substrate is removed and it could be extended to other transparent substrates. We have demonstrated that the transmittance, extracted from the blue channel of transmission mode optical images, monotonically depends on the number of layers. We have benchmarked the layer assignment done with this method with other extended spectroscopic techniques (micro-reflection, Raman, photoluminescence) finding an excellent agreement. Interestingly, this method is robust enough to provide an accurate layer determination even for samples with different doping level. In view of all this, the quantitative analysis of the transmission mode images can become a powerful method to select the flakes of 2D materials deposited onto transparent polymeric stamps prior to their deterministic transfer.

Experimental

Materials:

MoS₂ samples were prepared out of a bulk natural molybdenite crystal (Moly Hill mine, Quebec, Canada). MoSe₂ and WSe₂ samples were prepared out of bulk synthetic crystals grown by physical vapour transport method (provided by Prof. Rudolf Bratschitsch). WS₂ samples were prepared out of a bulk synthetic crystal grown by physical vapour transport method at Tennessee Crystal Center. The Fe-doped, Ni-doped, Nb-doped and Co-doped MoS₂ crystals were grown following the protocols described in Refs. [37–40]. A 0.5% of dopant material has been added during the synthesis of these doped MoS₂ samples which leads to a final doping level in the 0.3-0.4% range.

The transparent stamp substrate used in this work is a commercially available polydimethylsiloxane-based substrate manufactured by Gel-Pak® (Gel-Film® WF X4 6.0 mil). The TMDC flakes are exfoliated from the bulk crystals and transferred onto the surface of the Gel-Film stamp with a Nitto 224SPV adhesive tape.

Optical microscopy:

Optical microscopy images have been acquired with three different upright metallurgical microscopes, an AM Scope, a Motic BA MET310-T and a Nikon Eclipse CI, obtaining identical results. The transmission mode images have been acquired with an achromat condenser lens (N.A. 0.85) that ensures Köhler illumination, yielding to a homogeneous illumination spot of approximately 4 mm² on the sample. The light was collected with a 50x magnification plan achromatic objective (NA 0.55). Two different digital cameras were tested during this work, an AM Scope mu1803 camera with 18 megapixels and a Canon EOS 1200D, also providing identical results.

Image analysis:

The quantitative analysis of the transmittance of the flakes and the rippling wavelength has been carried out using Gwyddion® and ImageJ software.[46,47]

Acknowledgements

We thank Prof. Der-Yuh Lin and Prof. Tsung-Shine Ko for providing the doped MoS₂ samples. NT acknowledges to the Ministry of Science, Research and Technology of Iran. ACG and PG acknowledge funding from the European Commission Graphene Flagship (Grant Graphene Core 2 785219). RF acknowledges support from the Netherlands Organization for Scientific Research (NWO) through the research program Rubicon with project number 680-50-1515. ACG acknowledge funding from the European Research Council (ERC) under the European Union's Horizon 2020 research and innovation programme (grant agreement n° 755655, ERC-StG 2017 project 2D-TOPSENSE). D.-Y.L. acknowledges the financial support from the Ministry of Science and Technology of Taiwan, Republic of China under contract No. MOST 107-2112-M-018-002..

References

- [1] Novoselov, K.S.; Geim, A.K.; Morozov, S. V; Jiang, D.; Zhang, Y.; Dubonos, S. V; Grigorieva, I. V; Firsov, A.A. Electric Field Effect in Atomically Thin Carbon Films. *Science*, **2004**, *306*, 666–669.
- [2] Bonaccorso, F.; Lombardo, A.; Hasan, T.; Sun, Z.; Colombo, L.; Ferrari, A.C. Production and Processing of Graphene and 2d Crystals. *Mater. Today*, **2012**, *15*, 564–589.
- [3] Ferrari, A.C.; Bonaccorso, F.; Fal'ko, V.; Novoselov, K.S.; Roche, S.; Bøggild, P.; Borini, S.; Koppens, F.H.L.; Palermo, V.; Pugno, N.; Garrido, J.A.; Sordan, R.; Bianco, A.; Ballerini, L.; Prato, M.; Lidorikis, E.; Kivioja, J.; Marinelli, C.; Ryhänen, T.; Morpurgo, A.; Coleman, J.N.; Nicolosi, V.; Colombo, L.; Fert, A.; Garcia-Hernandez, M.; Bachtold, A.; Schneider, G.F.; Guinea, F.; Dekker, C.; Barbone, M.; Sun, Z.; Galiotis, C.; Grigorenko, A.N.; Konstantatos, G.; Kis, A.; Katsnelson, M.; Vandersypen, L.; Loiseau, A.; Morandi, V.; Neumaier, D.; Treossi, E.; Pellegrini, V.; Polini, M.; Tredicucci, A.; Williams, G.M.; Hee Hong, B.; Ahn, J.-H.; Min Kim, J.; Zirath, H.; van Wees, B.J.; van der Zant, H.; Occhipinti, L.; Di Matteo, A.; Kinloch, I.A.; Seyller, T.; Quesnel, E.; Feng, X.; Teo, K.; Rupesinghe, N.; Hakonen, P.; Neil, S.R.T.; Tannock, Q.; Löfwander, T.; Kinaret, J. Science and Technology Roadmap for Graphene, Related Two-Dimensional Crystals, and Hybrid Systems. *Nanoscale*, **2015**, *7*, 4598–4810.
- [4] Radisavljevic, B.; Radenovic, A.; Brivio, J.; Giacometti, V.; Kis, A. Single-Layer MoS₂ Transistors. *Nat. Nanotechnol.*, **2011**, *6*, 147–150.
- [5] Wang, Q.H.; Kalantar-Zadeh, K.; Kis, A.; Coleman, J.N.; Strano, M.S. Electronics and Optoelectronics of Two-Dimensional Transition Metal Dichalcogenides. *Nat. Nanotechnol.*, **2012**, *7*, 699–712.
- [6] Ni, Z.H.; Wang, H.M.; Kasim, J.; Fan, H.M.; Yu, T.; Wu, Y.H.; Feng, Y.P.; Shen, Z.X. Graphene Thickness Determination Using Reflection and Contrast Spectroscopy. *Nano Lett.*, **2007**, *7*, 2758–2763.
- [7] Inhwa Jung, †; Matthew Pelton, ‡; Richard Piner, †; Dmitriy A. Dikin, †; Sasha Stankovich, †; Supinda Watcharotone, †; Martina Hausner, § and; Rodney S. Ruoff*, †. Simple Approach for High-Contrast Optical Imaging and Characterization of Graphene-Based Sheets. **2007**.
- [8] Li, H.; Wu, J.; Huang, X.; Lu, G.; Yang, J.; Lu, X.; Xiong, Q.; Zhang, H. Rapid and Reliable Thickness Identification

of Two-Dimensional Nanosheets Using Optical Microscopy. *ACS Nano*, **2013**, *7*, 10344–10353.

- [9] Wang, X.; Zhao, M.; Nolte, D.D. Optical Contrast and Clarity of Graphene on an Arbitrary Substrate. *Appl. Phys. Lett.*, **2009**, *95*, 81102–31901.
- [10] Zhang, H.; Ran, F.; Shi, X.; Fang, X.; Wu, S.; Liu, Y.Y.; Zheng, X.; Yang, P.; Liu, Y.Y.; Wang, L.; Huang, X.; Li, H.; Huang, W. Optical Thickness Identification of Transition Metal Dichalcogenide Nanosheets on Transparent Substrates. *Nanotechnology*, **2017**, *28*, 164001.
- [11] Yu, Y.; Li, Z.; Wang, W.; Guo, X.; Jiang, J.; Nan, H.; Ni, Z. Investigation of Multilayer Domains in Large-Scale CVD Monolayer Graphene by Optical Imaging. *J. Semicond.*, **2017**, *38*, 33003.
- [12] Wang, Y.Y.; Gao, R.X.; Ni, Z.H.; He, H.; Guo, S.P.; Yang, H.P.; Cong, C.X.; Yu, T. Thickness Identification of Two-Dimensional Materials by Optical Imaging. *Nanotechnology*, **2012**, *23*, 495713.
- [13] Dean, C.R.; Young, A.F.; Meric, I.; Lee, C.; Wang, L.; Sorgenfrei, S.; Watanabe, K.; Taniguchi, T.; Kim, P.; Shepard, K.L.; Hone, J. Boron Nitride Substrates for High-Quality Graphene Electronics. *Nat. Nanotechnol.*, **2010**, *5*, 722–726.
- [14] Zomer, P.J.; Dash, S.P.; Tombros, N.; Van Wees, B.J. A Transfer Technique for High Mobility Graphene Devices on Commercially Available Hexagonal Boron Nitride. *Appl. Phys. Lett.*, **2011**, *99*, 232104.
- [15] Zomer, P.J.; Guimarães, M.H.D.; Brant, J.C.; Tombros, N.; Van Wees, B.J. Fast Pick up Technique for High Quality Heterostructures of Bilayer Graphene and Hexagonal Boron Nitride. *Appl. Phys. Lett.*, **2014**, *105*, 13101.
- [16] Castellanos-Gomez, A.; Buscema, M.; Molenaar, R.; Singh, V.; Janssen, L.; van der Zant, H.S.J.; Steele, G.A. Deterministic Transfer of Two-Dimensional Materials by All-Dry Viscoelastic Stamping. *2D Mater.*, **2014**, *1*, 011002.
- [17] Pizzocchero, F.; Gammelgaard, L.; Jessen, B.S.; Caridad, J.M.; Wang, L.; Hone, J.; Bøggild, P.; Booth, T.J. The Hot Pick-up Technique for Batch Assembly of van Der Waals Heterostructures. *Nat. Commun.*, **2016**, *7*, 11894.
- [18] Frisenda, R.; Navarro-Moratalla, E.; Gant, P.; De Lara, D.P.; Jarillo-Herrero, P.; Gorbachev, R. V.; Castellanos-Gomez, A. Recent Progress in the Assembly of Nanodevices and van Der Waals Heterostructures by Deterministic Placement of 2D Materials. *Chem. Soc. Rev.*, **2018**, *47*, 53–68.
- [19] Masubuchi, S.; Morimoto, M.; Morikawa, S.; Onodera, M.; Asakawa, Y.; Watanabe, K.; Taniguchi, T.; Machida, T. Autonomous Robotic Searching and Assembly of Two-Dimensional Crystals to Build van Der Waals Superlattices. *Nat. Commun.*, **2018**, *9*, 1413.
- [20] Liu, Y.; Weiss, N.O.; Duan, X.; Cheng, H.-C.; Huang, Y.; Duan, X. Van Der Waals Heterostructures and Devices. *Nat. Rev. Mater.*, **2016**, *1*, 16042.
- [21] Geim, A.K.; Grigorieva, I. V. Van Der Waals Heterostructures. *Nature*, **2013**, *499*, 419–425.
- [22] Novoselov, K.S.; Mishchenko, A.; Carvalho, A.; Castro Neto, A.H. 2D Materials and van Der Waals Heterostructures. *Science*, **2016**, *353*, aac9439.
- [23] Frisenda, R.; Molina-Mendoza, A.J.; Mueller, T.; Castellanos-Gomez, A.; van der Zant, H.S.J. Atomically Thin P–n Junctions Based on Two-Dimensional Materials. *Chem. Soc. Rev.*, **2018**, *47*, 3339–3358.
- [24] Splendiani, A.; Sun, L.; Zhang, Y.; Li, T.; Kim, J.; Chim, C.-Y.; Galli, G.; Wang, F. Emerging Photoluminescence in Monolayer MoS₂. *Nano Lett.*, **2010**, *10*, 1271–1275.
- [25] Pimenta, M.A.; del Corro, E.; Carvalho, B.R.; Fantini, C.; Malard, L.M. Comparative Study of Raman Spectroscopy in Graphene and MoS₂-Type Transition Metal Dichalcogenides. *Acc. Chem. Res.*, **2015**, *48*, 41–47.

- [26] Zhang, X.; Qiao, X.-F.; Shi, W.; Wu, J.-B.; Jiang, D.-S.; Tan, P.-H. Phonon and Raman Scattering of Two-Dimensional Transition Metal Dichalcogenides from Monolayer, Multilayer to Bulk Material. *Chem. Soc. Rev.*, **2015**, *44*, 2757–2785.
- [27] Zeng, H.; Cui, X. An Optical Spectroscopic Study on Two-Dimensional Group-VI Transition Metal Dichalcogenides. *Chem. Soc. Rev.*, **2015**, *44*, 2629–2642.
- [28] Frisenda, R.; Niu, Y.; Gant, P.; Molina-Mendoza, A.J.; Schmidt, R.; Bratschitsch, R.; Liu, J.; Fu, L.; Dumcenco, D.; Kis, A.; Perez De Lara, D.; Castellanos-Gomez, A. Micro-Reflectance and Transmittance Spectroscopy: A Versatile and Powerful Tool to Characterize 2D Materials. *J. Phys. D. Appl. Phys.*, **2017**, *50*, 074002.
- [29] Yang, R.; Zheng, X.; Wang, Z.; Miller, C.J.; Feng, P.X.-L. Multilayer MoS₂ Transistors Enabled by a Facile Dry-Transfer Technique and Thermal Annealing. *J. Vac. Sci. Technol. B, Nanotechnol. Microelectron. Mater. Process. Meas. Phenom.*, **2014**, *32*, 61203.
- [30] Castellanos-Gomez, A.; Quereda, J.; van der Meulen, H.P.; Agraït, N.; Rubio-Bollinger, G. Spatially Resolved Optical Absorption Spectroscopy of Single- and Few-Layer MoS₂ by Hyperspectral Imaging. *Nanotechnology*, **2016**, *27*, 115705.
- [31] Niu, Y.; Gonzalez-Abad, S.; Frisenda, R.; Marauhn, P.; Drüppel, M.; Gant, P.; Schmidt, R.; Taghavi, N.; Barcons, D.; Molina-Mendoza, A.; de Vasconcellos, S.; Bratschitsch, R.; Perez De Lara, D.; Röhlfing, M.; Castellanos-Gomez, A. Thickness-Dependent Differential Reflectance Spectra of Monolayer and Few-Layer MoS₂, MoSe₂, WS₂ and WSe₂. *Nanomaterials*, **2018**, *8*, 725.
- [32] Li, H.; Zhang, Q.; Yap, C.C.R.; Tay, B.K.; Edwin, T.H.T.; Olivier, A.; Baillargeat, D. From Bulk to Monolayer MoS₂: Evolution of Raman Scattering. *Adv. Funct. Mater.*, **2012**, *22*, 1385–1390.
- [33] Lee, C.; Yan, H.; Brus, L.E.; Heinz, T.F.; Hone, J.; Ryu, S. Anomalous Lattice Vibrations of Single- and Few-Layer MoS₂. *ACS Nano*, **2010**, *4*, 2695–2700.
- [34] Tonndorf, P.; Schmidt, R.; Böttger, P.; Zhang, X.; Börner, J.; Liebig, A.; Albrecht, M.; Kloc, C.; Gordan, O.; Zahn, D.R.T.; Michaelis de Vasconcellos, S.; Bratschitsch, R. Photoluminescence Emission and Raman Response of Monolayer MoS₂, MoSe₂, and WSe₂. *Opt. Express*, **2013**, *21*, 4908.
- [35] Mak, K.F.; Lee, C.; Hone, J.; Shan, J.; Heinz, T.F. Atomically Thin MoS₂: A New Direct-Gap Semiconductor. *Phys. Rev. Lett.*, **2010**, *105*, 2–5.
- [36] Splendiani, A.; Sun, L.; Zhang, Y.; Li, T.; Kim, J.; Chim, C.-Y.; Galli, G.; Wang, F. Emerging Photoluminescence in Monolayer MoS₂. *Nano Lett.*, **2010**, *10*, 1271–1275.
- [37] Suh, J.; Park, T.-E.; Lin, D.-Y.; Fu, D.; Park, J.; Jung, H.J.; Chen, Y.; Ko, C.; Jang, C.; Sun, Y. Doping against the Native Propensity of MoS₂: Degenerate Hole Doping by Cation Substitution. *Nano Lett.*, **2014**, *14*, 6976–6982.
- [38] Svatek, S.A.; Antolin, E.; Lin, D.-Y.; Frisenda, R.; Reuter, C.; Molina-Mendoza, A.J.; Muñoz, M.; Agraït, N.; Ko, T.-S.; de Lara, D.P.; Castellanos-Gomez, A. Gate Tunable Photovoltaic Effect in MoS₂ Vertical P–n Homostructures. *J. Mater. Chem. C*, **2017**, *5*, 854–861.
- [39] Reuter, C.; Frisenda, R.; Lin, D.-Y.; Ko, T.-S.; Perez de Lara, D.; Castellanos-Gomez, A. A Versatile Scanning Photocurrent Mapping System to Characterize Optoelectronic Devices Based on 2D Materials. *Small Methods*, **2017**, *1*, 1700119.
- [40] Wang, S.Y.; Ko, T.S.; Huang, C.C.; Huang, Y.S. Optical and Electrical Properties of MoS₂ and Fe-Doped MoS₂. *Jpn. J. Appl. Phys.*, **2014**, *53*, 04EH07.
- [41] Chen, Y.; Dumcenco, D.O.; Zhu, Y.; Zhang, X.; Mao, N.; Feng, Q.; Zhang, M.; Zhang, J.; Tan, P.-H.; Huang,

Y.-S. Composition-Dependent Raman Modes of Mo_{1-x}W_xS₂ Monolayer Alloys. *Nanoscale*, **2014**, *6*, 2833–2839.

- [42] Dumcenco, D.O.; Kobayashi, H.; Liu, Z.; Huang, Y.-S.; Suenaga, K. Visualization and Quantification of Transition Metal Atomic Mixing in Mo_{1-x}W_xS₂ Single Layers. *Nat. Commun.*, **2013**, *4*, 1351.
- [43] Mann, J.; Ma, Q.; Odenthal, P.M.; Isarraraz, M.; Le, D.; Preciado, E.; Barroso, D.; Yamaguchi, K.; von Son Palacio, G.; Nguyen, A. 2-Dimensional Transition Metal Dichalcogenides with Tunable Direct Band Gaps: MoS₂ (1-x)Se_{2x} Monolayers. *Adv. Mater.*, **2014**, *26*, 1399–1404.
- [44] Zhang, M.; Wu, J.; Zhu, Y.; Dumcenco, D.O.; Hong, J.; Mao, N.; Deng, S.; Chen, Y.; Yang, Y.; Jin, C. Two-Dimensional Molybdenum Tungsten Diselenide Alloys: Photoluminescence, Raman Scattering, and Electrical Transport. *ACS Nano*, **2014**, *8*, 7130–7137.
- [45] Mouri, S.; Miyauchi, Y.; Matsuda, K. Tunable Photoluminescence of Monolayer MoS₂ via Chemical Doping. *Nano Lett.*, **2013**, *13*, 5944–5948.
- [46] Nečas, D.; Klapetek, P. Gwyddion: An Open-Source Software for SPM Data Analysis. *Open Phys.*, **2012**, *10*, 181–188.
- [47] Abràmoff, M.D.; Magalhães, P.J.; Ram, S.J. Image Processing with ImageJ. *Biophotonics Int.*, **2004**, *11*, 36–42.

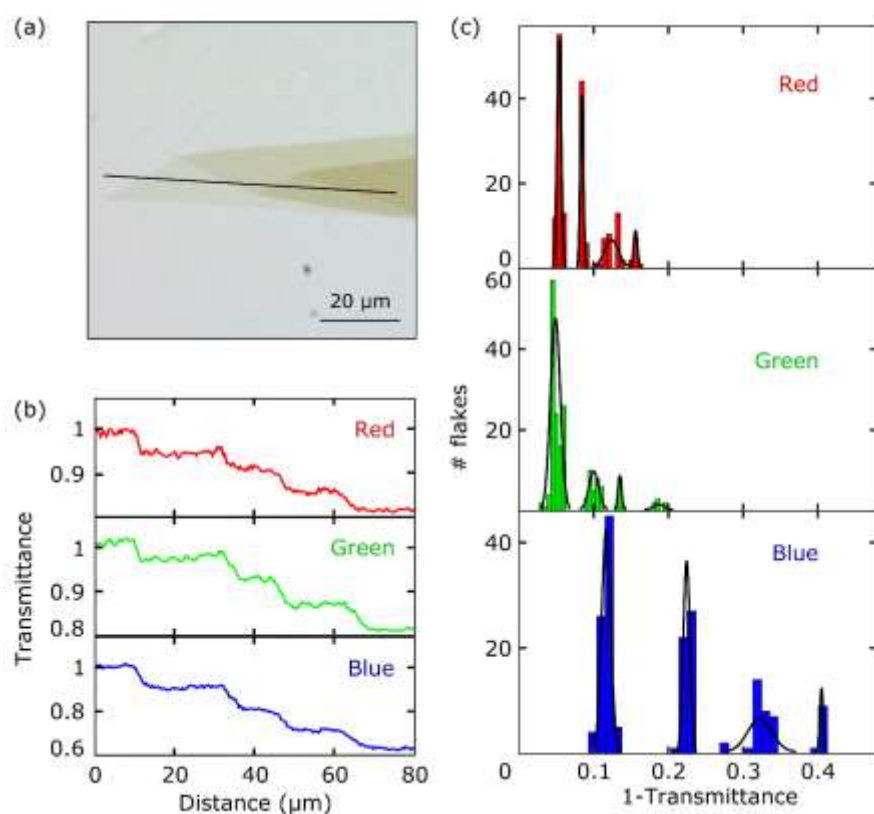


Figure 1. (a) Optical image in transmission mode of a MoS₂ flake with different thicknesses. (b) Line profiles of the intensities of the red, green and blue channels of the image in 1a. (c) Histograms of the 1-transmittance value in the RGB channels for several MoS₂ flakes.

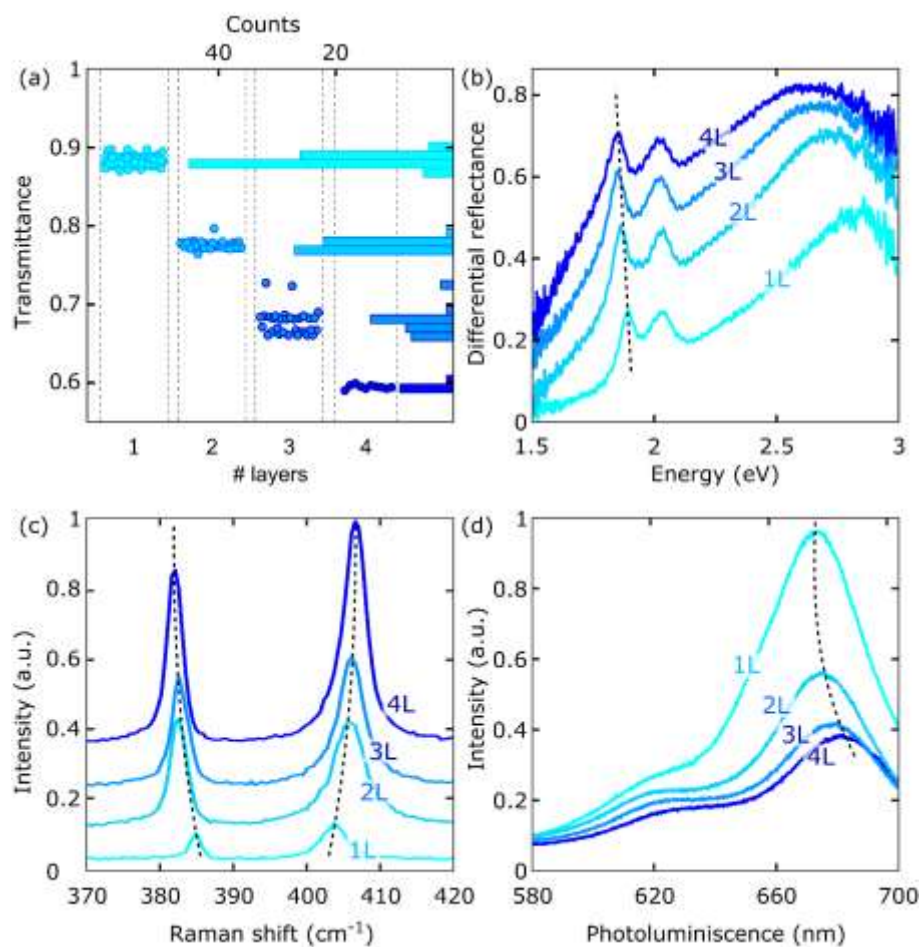


Figure 2. (a) Scatter plot and histogram of the blue channel transmission values for several MoS₂ flakes. (b) Differential reflectance spectra for MoS₂ with different number of layers. (c) Raman spectra for MoS₂ with different number of layers. (d) Photoluminescence of MoS₂ for different number of layers.

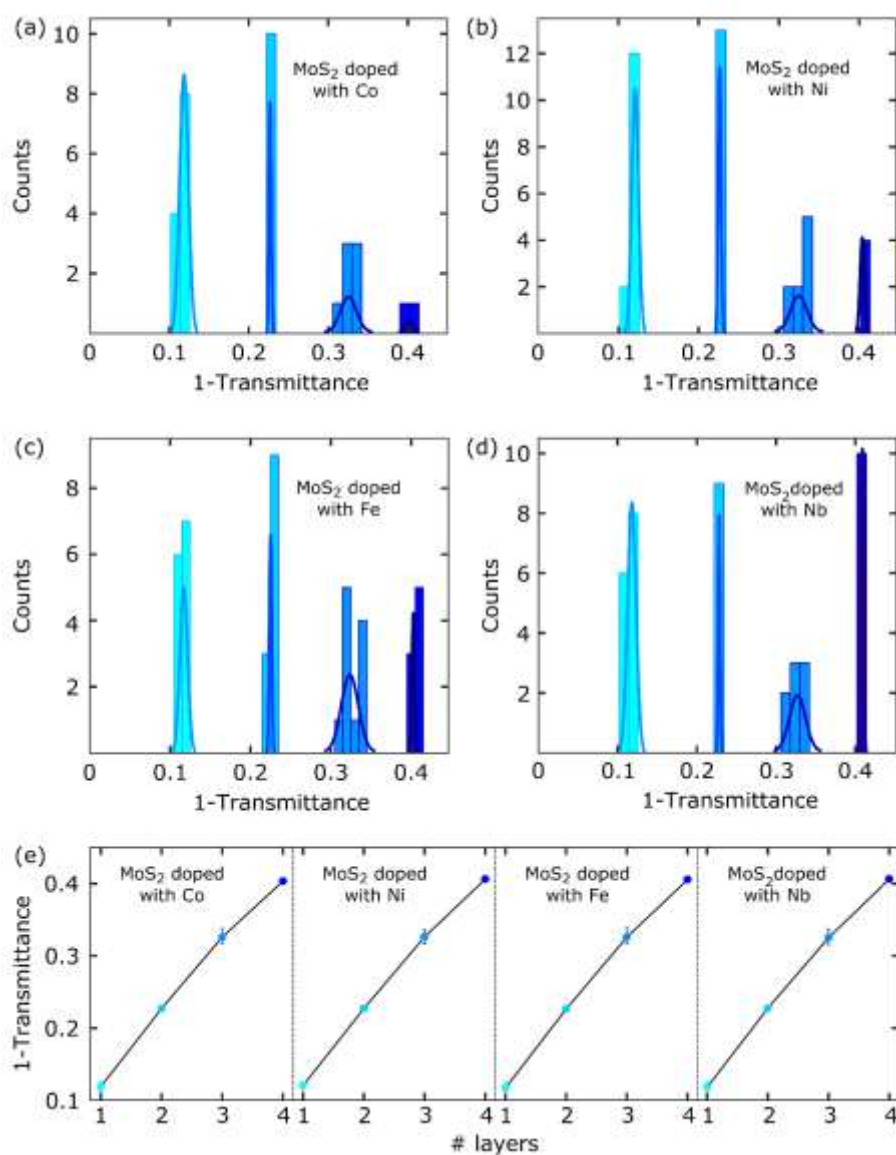


Figure 3. Histograms of the 1-transmission value in the blue channel for MoS₂ flakes doped with (a) Co, (b) Ni, (c) Fe and (d) Nb. (e) Average of the 1-transmission values for 1L to 4L in each material.

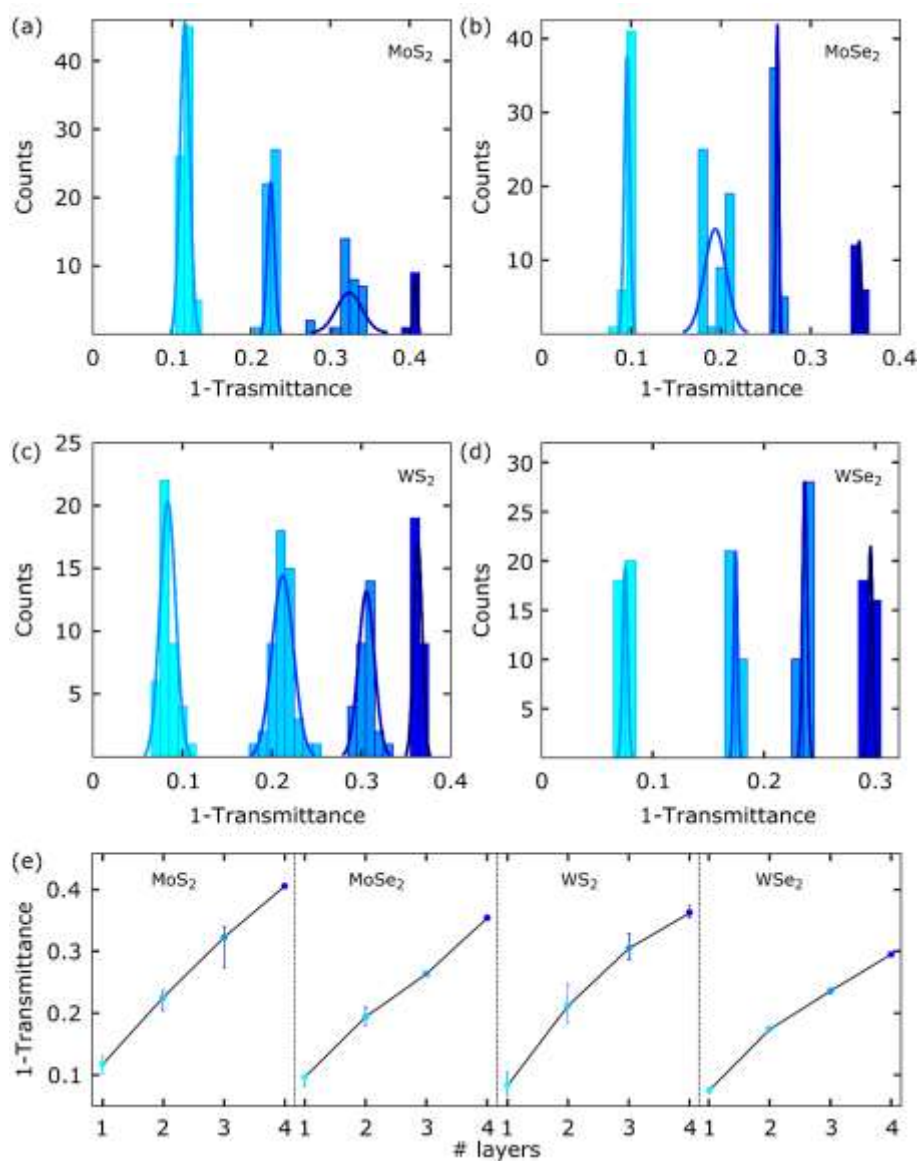


Figure 4. Histograms of the 1-transmittance value in the blue channel for (a) MoS₂, (b) MoSe₂, (c) WS₂ and (d) WSe₂ flakes. (e) Average of the 1-transmittance values for 1L to 4L in each material.

Electronic Supplementary Material

Thickness determination of MoS₂, MoSe₂, WS₂ and WSe₂ on transparent stamps used for deterministic transfer of 2D materials

Najme S. Taghavi^{1,2}, Patricia Gant¹(✉), Peng Huang^{1,3}, Iris Niehues⁴, Robert Schmidt⁴, Steffen Michaelis de Vasconcellos⁴, Rudolf Bratschitsch⁴, Mar García-Hernández¹, Riccardo Frisenda¹(✉), Andres Castellanos-Gomez¹(✉)

¹ Materials Science Factory, Instituto de Ciencia de Materiales de Madrid (ICMM), Consejo Superior de Investigaciones Científicas (CSIC), Sor Juana Inés de la Cruz 3, 28049 Madrid, Spain.

² Faculty of Physics, Khaje Nasir Toosi University of Technology (KNTU), Tehrān 19697 64499, Iran.

³ State Key Laboratory of Tribology, Tsinghua University, Beijing 100084, China.

⁴ Institute of Physics and Center for Nanotechnology, University of Münster, 48149 Münster, Germany.

Address correspondence to Patricia Gant (patricia.gant@csic.es), Riccardo Frisenda (riccardo.frisenda@csic.es) and Andres Castellanos-Gomez (andres.castellanos@csic.es)

INFORMATION ABOUT ELECTRONIC SUPPLEMENTARY MATERIAL.

1. Constructing a thickness map from transmission mode optical microscopy image
2. Blue channel transmittance for flakes thicker than 4 layers

Constructing a thickness map from transmission mode optical microscopy image

Interestingly one can directly convert a transmission mode optical microscopy image into a thickness map by using this quantitative analysis of the blue channel. First, the blue channel of the transmission mode image is extracted and the average intensity of the substrate (T_0) is measured. Then, we calculate $1-T/T_0$ to each pixel of the blue channel image, where T is the blue intensity at each pixel of the image. Under such transformation the substrate value becomes ~ 0 and the value on the flakes can be directly compared to the values in the histograms displayed in Figure 4. Indeed, by selecting a colormap accordingly to the $1-T/T_0$ histograms in Figure 4 the map directly displays the number of layers.

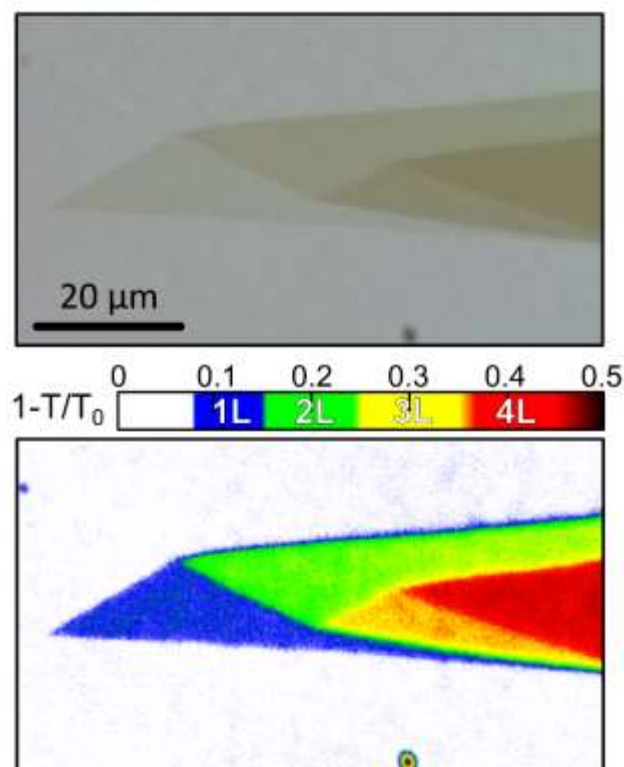


Figure S1. Transformation of a transmission mode optical microscopy image (top) into a thickness map (bottom) by applying the formula $1-T/T_0$, where T is the intensity of each pixel and T_0 is the average intensity of the substrate. By selecting a colormap accordingly to the $1-T/T_0$ histograms in Figure 4 the map displays the number of layers.

Blue channel transmittance for flakes thicker than 4 layers

In the main text we focused on the analysis of the transmittance of flakes 1L to 4L thick because we had plenty of statistics in that thickness range and because we used complementary techniques like Raman spectroscopy, photoluminescence and micro-reflectance/transmittance to double-check the assessed number of layers. The uncertainty of the number of layers assessment done by those techniques increases substantially for flakes thicker than 4-5 layers. Figure S2 shows the analysis of the transmittance of the blue channel for TMDC flakes thicker than 4 layers.

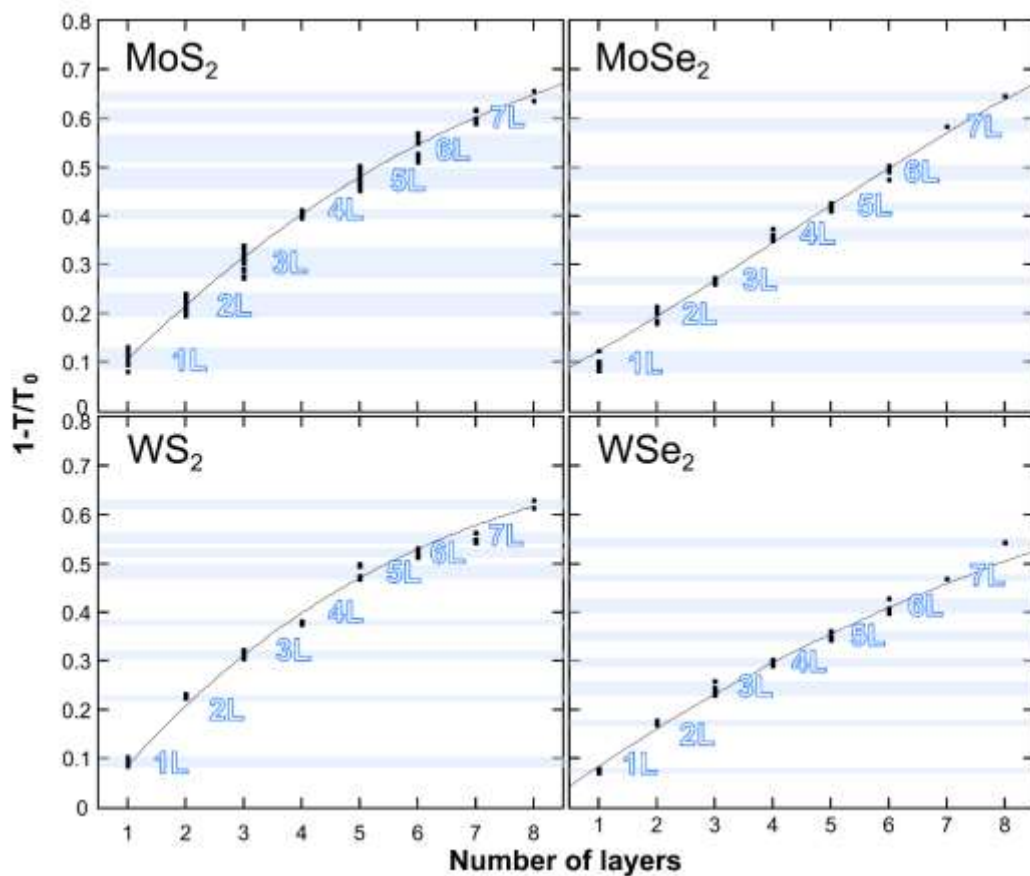


Figure S2. 1 - transmittance of the blue channel measured for MoS₂, MoSe₂, WS₂ and WSe₂ flakes with thicknesses in the range of 1L to 8L.